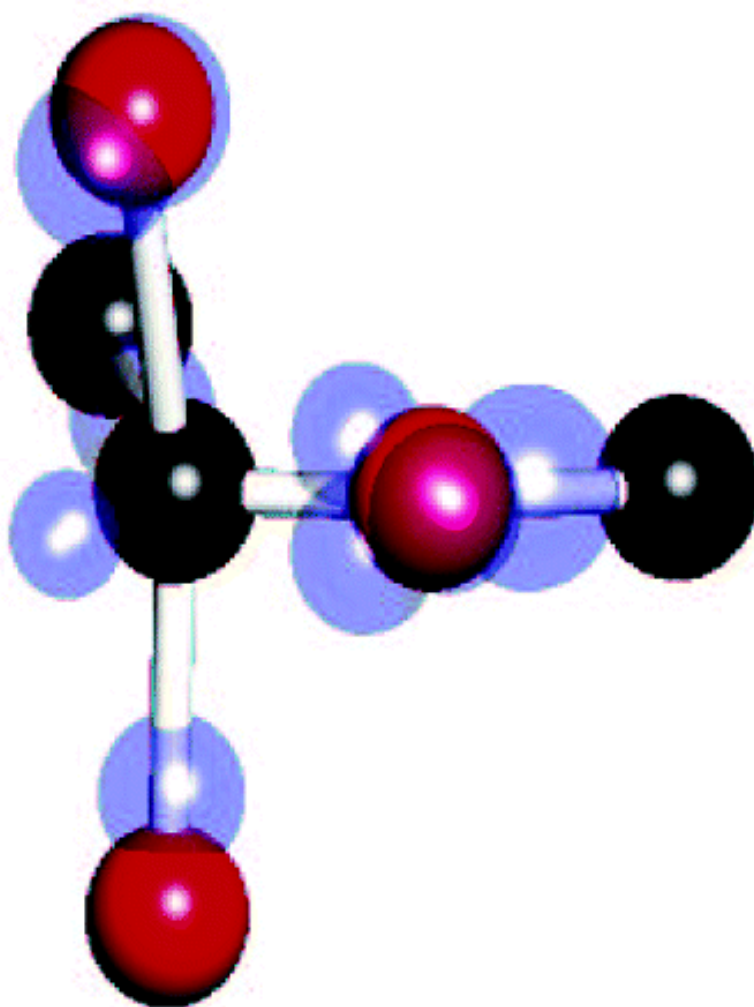


## Glycosidic Bond Formation in Aqueous Solution: On the Oxocarbenium Intermediate

John M. Stubbs, and Dominik Marx

*J. Am. Chem. Soc.*, **2003**, 125 (36), 10960-10962 • DOI: 10.1021/ja035600n • Publication Date (Web): 15 August 2003

Downloaded from <http://pubs.acs.org> on March 29, 2009



### More About This Article

---



ACS Publications  
High quality. High impact.

Additional resources and features associated with this article are available within the HTML version:

- Supporting Information
- Links to the 1 articles that cite this article, as of the time of this article download
- Access to high resolution figures
- Links to articles and content related to this article
- Copyright permission to reproduce figures and/or text from this article

[View the Full Text HTML](#)



## Glycosidic Bond Formation in Aqueous Solution: On the Oxocarbenium Intermediate

John M. Stubbs\*<sup>†</sup> and Dominik Marx

Contribution from Lehrstuhl für Theoretische Chemie, Ruhr-Universität Bochum,  
44780 Bochum, Germany

Received April 12, 2003; E-mail: stubbs@chem.umn.edu

**Abstract:** The mechanism of specific acid-catalyzed glycosidic bond formation between methanol and  $\alpha$ -D-glucopyranoside in aqueous solution at 300 K was studied using Car–Parrinello molecular dynamics. The reaction was found to proceed through a non-solvent equilibrated oxocarbenium cation intermediate characterized by the loss of a hydrogen-bonding interaction between the ring oxygen and solvating water. The mechanism, which was found to be  $D_N^*A_N$  in nature, is discussed in detail.

### Introduction

The glycosidic bond is of fundamental importance to many aspects of chemistry and biology, forming the basis of carbohydrate chemistry. Because of its prominent appearance in digestion and sensitivity to many factors, it is not surprising that glycosidic bond solvolysis has been studied extensively experimentally.<sup>1–11</sup> The hydrolysis reaction mechanism of glucopyranosides has been concluded to be dissociative ( $D_N+A_N$ , see ref 12 for definitions) or partially dissociative with a short-lived intermediate<sup>1–5</sup> ( $D_N^*A_N$ ), although a concerted mechanism<sup>6</sup> ( $A_ND_N$ ) has also been observed. The hydrolysis mechanism is thought to provide insufficient time for the oxocarbenium ion intermediate to become solvent equilibrated, with an estimated lifetime<sup>2,9</sup> of  $\sim 1$ –3 ps. Although glycosidic bond formation is also of crucial importance, e.g. in terms of polysaccharide synthesis, it is not much studied.

Previous theoretical treatments have focused mainly on aspects of reactivity and conformational stability of mono- or disaccharides using quantum chemical gas phase or continuum solvation methods,<sup>13–15</sup> with notable exceptions investigating

uracil-DNA glycosylase via a QM/MM approach<sup>16</sup> and glycosyltransferase via a QM potential energy surface approach.<sup>17</sup> Others have focused on the solvation and hydrogen-bonding behavior without studying chemical reactions using molecular dynamics methods.<sup>18</sup> By combining these findings it can be anticipated that the presence of water will be critical for the mechanism so that condensed-phase results are expected to differ substantially from gas-phase results. Until now, neither hydrolysis nor glycosylation have been investigated in solution.

### Results and Discussion

Here, we study theoretically the acid-catalyzed glycosidic bond formation between  $\alpha$ -D-glucopyranose and methanol at “wet chemistry conditions”. To this end Car–Parrinello ab initio molecular dynamics simulations<sup>19</sup> were carried out. An initial configuration was prepared by very slowly pushing the O<sup>m</sup> atom of methanol to the C<sup>1</sup> site on the sugar ring in a large simulation cell using a force field. At a distance constraint of 2.7 Å a proton was added, the ab initio run was initialized keeping 57 water molecules to solvate the reactive complex, and a Nosé–Hoover temperature of 300 K was established. Trouiller–Martins norm-conserving pseudopotentials<sup>19</sup> were employed together with the BLYP functional, a plane wave cutoff of 70 Ry at the  $\Gamma$ -point in a periodic cubic 12.255 Å supercell, and as usual hydrogen was substituted by deuterium to allow for a larger MD time step.<sup>19b</sup> Only for convenience, events during the simulation will be referred to according to the time at which they occurred;

<sup>†</sup> On leave from: Department of Chemistry, University of Minnesota, Minneapolis, MN 55455-0431.

- (1) Bennet, A. J.; Sinnott, M. L. *J. Am. Chem. Soc.* **1986**, *108*, 7287.
- (2) (a) Zhu, J.; Bennet, A. J. *J. Am. Chem. Soc.* **1998**, *120*, 3887. (b) Huang, X.; Surry, C.; Hiebert, T.; Bennet, A. J. *J. Am. Chem. Soc.* **1995**, *117*, 10614.
- (3) Namchuk, M. N.; McCarter, J. D.; Becalski, A.; Andrews, T.; Withers, S. G. *J. Am. Chem. Soc.* **2000**, *122*, 1270.
- (4) Indurugalla, D.; Bennet, A. J. *J. Am. Chem. Soc.* **2001**, *123*, 10889.
- (5) Zhu, J.; Bennet, A. J. *J. Org. Chem.* **2000**, *65*, 4423.
- (6) (a) Zhang, Y.; Bommsuwamy, J.; Sinnott, M. L. *J. Am. Chem. Soc.* **1994**, *116*, 7557. (b) Banait, N. S.; Jencks, W. P. *J. Am. Chem. Soc.* **1991**, *113*, 7951.
- (7) Bennet, A. J.; Kitos, T. E. *J. Chem. Soc., Perkin Trans. 2* **2002**, 1207.
- (8) Richard, J. P.; Jencks, W. P. *J. Am. Chem. Soc.* **1984**, *106*, 1373.
- (9) Amyes, T. L.; Jencks, W. P. *J. Am. Chem. Soc.* **1989**, *111*, 7888.
- (10) Bennet, A. J.; Davis, A. J.; Hosie, L.; Sinnott, M. L. *J. Chem. Soc., Perkin Trans. 2* **1987**, 581.
- (11) Sinnott, M. L.; Jencks, W. P. *J. Am. Chem. Soc.* **1980**, *102*, 2026.
- (12) (a) Guthrie, R. D. *Pure Appl. Chem.* **1989**, *61*, 23. (b) Guthrie, R. D.; Jencks, W. P. *Acc. Chem. Res.* **1989**, *22*, 343.
- (13) Andrews, C. W.; Fraser-Reid, B.; Bowen, J. P. *J. Am. Chem. Soc.* **1991**, *113*, 8293.
- (14) Buckley, N.; Oppenheimer, N. J. *J. Org. Chem.* **1996**, *61*, 8048.

- (15) (a) Barrows, S. E.; Storer, J. W.; Cramer, C. J.; French, A. D.; Truhlar, D. G. *J. Comput. Chem.* **1998**, *19*, 1111. (b) Smith, B. J. *J. Am. Chem. Soc.* **1997**, *119*, 2699. (c) Bérces, A.; Enright, G.; Nukada, T.; Whitfield, D. M. *J. Am. Chem. Soc.* **2001**, *123*, 5460.
- (16) Dinner, A. R.; Blackburn, G. M.; Karplus, M. *Nature* **2001**, *413*, 752.
- (17) Tvaroska, I.; André, I.; Carver, J. P. *J. Am. Chem. Soc.* **2000**, *122*, 8762.
- (18) (a) Molteni, C.; Parrinello, M. *J. Am. Chem. Soc.* **1998**, *120*, 2168. (b) Naidoo, K. J.; Brady, J. W. *J. Am. Chem. Soc.* **1999**, *121*, 2244. (c) Vishnyakov, A.; Widmalm, G.; Kowalewski, J.; Laaksonen, A. *J. Am. Chem. Soc.* **1999**, *121*, 5403.
- (19) (a) Car, R.; Parrinello, M. *Phys. Rev. Lett.* **1985**, *55*, 2471. (b) Marx, D.; Hutter, J. In *Modern Methods and Algorithms of Quantum Chemistry*; J. Grotendorst, J., Ed.; NIC, FZ: Jülich, 2000; p 301–449; see www.theochem.ruhr-uni-bochum.de/go/cprev.html. (c) CPMD, Hutter, J. et al., MPI FKF and IBM Zurich.

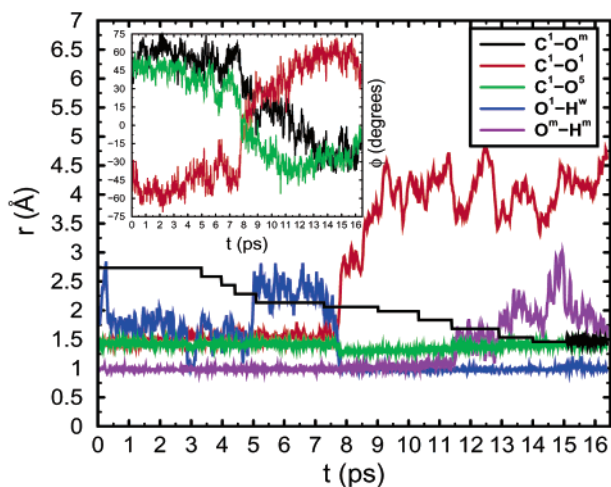


**Figure 1.** Evolution of distances as the  $C^1-O^m$  constraint is decreased from 2.689 Å at  $t = 0$  ps to 1.462 Å at  $t = 15$  ps where unconstrained dynamics sets in. Black, red, green, blue, and purple lines represent  $C^1-O^m$ ,  $C^1-O^1$ ,  $C^1-O^5$ ,  $O^1-H^w$ , and  $O^m-H^m$  distances, respectively. Inset depicts the three changing endocyclic torsional angles where black, red, and green represent  $C^4-C^5-O^5-C^1$ ,  $C^5-O^5-C^1-C^2$ , and  $O^5-C^1-C^2-C^3$  angles, respectively.

however, it must be emphasized that due to the constraint this should not be interpreted as real time. Because of the very nature of the simulation it is not possible to determine where the exact transition state is; thus, strict comparisons to kinetic isotope effect (KIE) data should be made with caution. Additionally, due to computational expense only a single reaction path, inversion of the anomeric configuration, was investigated as it leads to the generally favored stereoproduct.<sup>5,11</sup>

A first impression of the mechanism can be inferred from the atomic separations plotted in Figure 1, which shows the formation of methyl  $\beta$ -D-glucopyranoside occurring in two sequential steps as the  $C^1-O^m$  distance (black line) is decreased. The first one (I) consists of concerted protonation of  $O^1$  in the leaving hydroxyl group (blue), breaking of the  $C^1-O^1$  bond (red), and shortening of the  $C^1-O^5$  bond (green) within the sugar ring close to 7.76 ps initiated by irreversible protonation of  $O^1$  which changes the orientation of the attacking methanol as evidenced by the  $O^5-C^1-O^m$  angle moving from 80 to 100°, see Figure 2a  $\rightarrow$  b. Step II involves the formation of the new  $C^1-O^m$  bond (black), deprotonation of  $O^m$  (violet) and an increase in the  $C^1-O^5$  bond length (green), see Figure 2c  $\rightarrow$  d. Prior to step I, two protonations of the leaving hydroxyl group, i.e., of  $O^1$ , at about 3.0 and 4.7 ps were unsuccessful in cleaving the  $C^1-O^1$  covalent bond, which implies that it was necessary to have the methanol  $O^m$  sufficiently close to  $C^1$  before dehydration could occur. This points away from the intermediate cation having sufficient time to become solvent equilibrated before the  $C^1-O^m$  bond is formed, similar to glycosyltransferase mechanisms with close proximity of the nucleophile before ionization.<sup>17</sup> Each reversible protonation of  $O^1$  was followed by a corresponding increase in  $C^1-O^1$  and decrease in  $C^1-O^5$  bond lengths, most noticeable in Figure 1 at 3.0 ps, characteristic both of specific acid catalysis<sup>1,20</sup> and the near synchronicity of step I. The coupling of  $C^1-O^5$  bond shortening and  $C^1-O^1$  bond breaking is at odds with KIE data for the hydrolysis of methyl  $\alpha$ - and  $\beta$ -D-glucopyranoside<sup>1</sup> which indicates a delay between

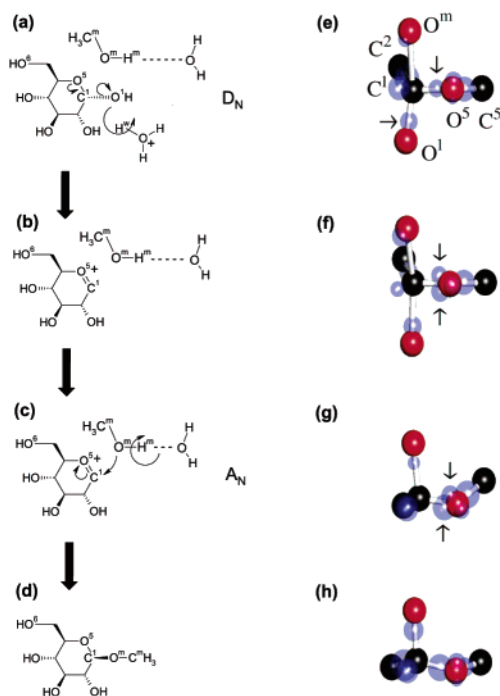


**Figure 2.** Scheme of the reaction mechanism (a–d) and ball-and-stick representation of the most important atoms (O: red, C: black) in representative trajectory snapshots taken at 7.27 ps (e), 7.74 ps (f), 12.5 ps (g), and 13.5 ps (h). The Wannier centers are represented by transparent spheres (blue) with radii being proportional to the spread of the localized orbitals.

the two events, although the same hydrolysis reaction for methyl xylopyranosides<sup>4</sup> is known to be simultaneous. A further simulation study on xylopyranosides could potentially shed light on this difference. The three endocyclic ring torsional angles that change throughout the simulation are depicted in the inset of Figure 1 which shows the change from the initial  ${}^4C_1$  to the final predominantly  ${}^1S_3$  twist boat structure occurring continuously starting at 7.76 ps.

Once the  $C^1-O^m$  distance has reached 2.06 Å at 7.27 ps, it takes about 500 fs until the  $C^1-O^5$  bond length contracts abruptly by as much as  $\sim 0.15$  Å. The chemistry responsible becomes obvious upon analyzing the electronic structure by localizing the canonical Bloch orbitals in terms of Wannier functions.<sup>21</sup> In Figure 2e, corresponding to the normal  $C^1-O^5$  bond length, one can identify two Wannier centers (i.e. average positions of appropriate Wannier orbitals) representing the two lone pairs at  $O^5$ . In addition there is one center each on the connecting axes to the neighboring carbon atoms  $C^1$  and  $C^5$ , which indicates two C–O single bonds (see arrows). This bonding pattern changes *qualitatively* once the  $C^1-O^5$  bond contracts: there is only one lone pair left at  $O^5$ , and two Wannier centers become aligned along the  $C^1-O^5$  axis, see Figure 2f and arrows therein. In terms of a simple Lewis picture this clearly implies the formation of a  $C^1=O^5$  double bond at 7.7 ps, i.e., of an oxocarbenium cation, which with the incoming methanol molecule forms an ion:dipole complex and remains stable up to about 11.4 ps. This localized orbital analysis was confirmed by a more elaborate investigation (not depicted) of the electron localization function (ELF); see ref 22 for a review.

(21) Marzari, N.; Vanderbilt, D. *Phys. Rev. B* **1997**, *56*, 12847; note that Wannier functions correspond to Boys' localized orbitals for finite systems such as isolated molecules.

(20) Capon, B. *Chem. Rev.* **1969**, *69*, 407.

Here, clear evidence for oxocarbenium formation is found in terms of the emergence of a double bond attractor between C<sup>1</sup> and O<sup>5</sup> in conjunction with only one lone pair attractor left at O<sup>5</sup>. Most interestingly, it is observed by analyzing coordination numbers (not shown) that O<sup>1</sup> expels a solvating water at about 8 ps, remains “unsolvated” during the oxocarbenium reign, and partially reestablishes a hydrogen bond to *another* water at ~11.4 ps.

Between approximately 11.4 and 12.9 ps, at a constant C<sup>1</sup>–O<sup>m</sup> distance of 1.69 Å, several deprotonation attempts of O<sup>m</sup> occur, each of which manifests itself by an increase of the C<sup>1</sup>–O<sup>5</sup> bond. In this period the Wannier centers of O<sup>5</sup>, see Figure 2g, are found to oscillate between one or two lone pairs and a double or single C<sup>1</sup>–O<sup>5</sup> bond, respectively, see arrows. During this period the C<sup>1</sup> carbon is mostly rehybridized back to sp<sup>3</sup>. Finally, when the C<sup>1</sup>–O<sup>m</sup> distance is reduced to 1.54 Å, which lies at the edge of the fluctuating range of bond lengths in the subsequent unconstrained simulation after 15.0 ps, the O<sup>m</sup> oxygen is definitely deprotonated, the C<sup>1</sup>–O<sup>5</sup> bond length returns to the typical single-bond value, see Figure 2h, and a hydrogen bond is again fully accepted by O<sup>5</sup>.

From the force acting on the constraint the free energy of the reaction can be calculated<sup>19</sup> along this reaction coordinate. The difference between the reactant and product energies is 25 kcal mol<sup>-1</sup> with a barrier height of 35 kcal mol<sup>-1</sup> to formation. The transition state, which coincides both with the maximum in the free energy profile and step I, can be located around 7.7 ps, see Figure 2f. It is likely that a general base would lower the reaction barrier height by facilitating the removal of the H<sup>m</sup> hydrogen. Upon inspection of the pyranose conformation it is apparent the transition state is predominantly a <sup>4</sup>C<sub>1</sub> chair conformation with a noticeable amount of <sup>1</sup>S<sub>5</sub> character which is similar to the proposed transition state for the corresponding hydrolysis.<sup>1,2,7</sup> At the transition state the C<sup>1</sup>–O<sup>1</sup> distance was ~1.9 Å indicating the degree of bond cleavage is almost complete. As the starting conformation of the pyranose ring was

also <sup>4</sup>C<sub>1</sub> the transition state must be regarded as an early one, which is consistent with a late transition state for the back reaction.<sup>1,6</sup> Unlike the gas-phase calculations<sup>14</sup> for the transition state of protonated methyl-β-D-glucopyranoside, which predict a stabilizing *intramolecular* interaction of the protonated O<sup>m</sup> by O<sup>6</sup>, our condensed-phase simulations find a solvent water in this role instead – which was not available in the gas-phase calculations.

## Conclusions

In summary, the specific acid-catalyzed reaction of methanol and α-D-glucopyranose is found to proceed via a D<sub>N</sub>\*A<sub>N</sub> mechanism just as the hydrolysis of methyl α- and β-D-glucopyranoside.<sup>1</sup> The D<sub>N</sub> step consists of a concerted protonation of the O<sup>1</sup> hydroxyl group, breaking of the C<sup>1</sup>–O<sup>1</sup> bond and oxocarbenium ion formation involving C<sup>1</sup>=O<sup>5</sup>. The second A<sub>N</sub> part is the making of the C<sup>1</sup>–O<sup>m</sup> glycosidic bond, deprotonation of the methanol hydroxyl group O<sup>m</sup>H<sup>m</sup>, and reformation of the C<sup>1</sup>–O<sup>5</sup> single bond. The oxocarbenium intermediate, which exists between the D<sub>N</sub> and A<sub>N</sub> events, is nonsolvent equilibrated in light of the apparent necessity of a close approach of the methanol O<sup>m</sup> before its formation. This was also found to be the case for many glucopyranoside hydrolysis reactions,<sup>1,2</sup> as well as for a theoretical study of glycosyltransferase.<sup>17</sup> The stabilization of this carbocation results in the loss of a hydrogen bonding interaction involving O<sup>5</sup>, which is reestablished right at the formation of the new C<sup>1</sup>–O<sup>m</sup> bond.

**Acknowledgment.** We are indebted to J. I. Siepmann for his support, and we are grateful to R. Rousseau and N. Doltsinis for discussions. The calculations were carried out at the Minnesota Supercomputing Institute and at BOVILAB@RUB (Bochum). We thank the German Academic Exchange Program (DAAD), the Graduate School for a Frieda Martha Kunze Fellowship, the National Science Foundation (CTS-0138393), FOR 436, and FCI for financial support.

JA035600N

(22) Savin, A.; Nesper, R.; Wengert, S.; Fässler, T. F. *Angew. Chem.* **1997**, *109*, 1892; *Angew. Chem., Int. Ed. Engl.* **1997**, *36*, 1808.